Interaction Between Normal and Shear Stresses and Its Effect on Multiaxial Fatigue Behavior

Shahriar Sharifimehr[1,1], *Ali* Fatemi[2]

[1]Mechanical, Industrial, and Manufacturing Engineering, University of Toledo, Toledo, Ohio, USA
[2]Mechanical Engineering Department, University of Memphis, Memphis, Tennessee, USA

Abstract. Interaction between normal and shear stresses plays an important role in multiaxial fatigue damage. The aim of this study was to investigate this interaction effect on fatigue behavior of shear failure mode materials under multiaxial loading conditions. In order to model the influence of normal stress on fatigue damage, the present study introduces a method based on the idea that the normal stress acting on the critical plane orientation causes two types of influence, first by affecting roughness induced closure, and second, by a fluctuating normal stress affecting the growth of small cracks in mode II. The summation of these terms could then be used in shear-based critical plane damage models, for example FS damage model, which use normal stress as a secondary input. In order to investigate the effect of the method, constant amplitude load paths with different levels of interaction between the normal and shear stresses were designed for an experimental program. The proposed method was observed to result in improved fatigue life estimations where significant interactions between normal and shear stresses exist.

1 Introduction

In materials with shear failure mode, although cyclic shear strain on the failure plane is primarily controlling crack initiation, the normal stress acting on the failure plane can significantly affect the crack initiation process [1]. A tensile normal stress on the critical plane can reduce the friction between the faces of a small crack by holding the faces of the small crack open and, therefore, accelerating the crack initiation. On the other hand, a compressive normal stress on the critical plane can cause retardation in this process.

Therefore, the interaction between these stresses is an important factor in the fatigue analysis process and can influence the amount of fatigue damage. The role of interaction between normal and shear stresses is especially important in fatigue behavior under service loading conditions where the state of stress is often multiaxial and the loading histories are non-proportional. These types of histories have varying levels of interaction between normal and shear stresses throughout the life of the component.

A number of studies have investigated the effect of interactions between normal and shear forces on fatigue behavior. For instance, Wu and Yang [2] studied the effect of interaction

1 Corresponding author: shahriar.sharifimehr@rockets.utoledo.edu

between tensile and shear strains by testing 304 stainless steel under two paths with different interactions of tensile and shear strains. They observed that with the same amounts of tensile and shear strain, the path with higher interaction resulted in shorter lives by a factor of about two compared to the other. Kurath et al. [3] used the FS damage parameter to analyze the results of tests on SAE 1045 steel specimens under four paths with different amounts of interaction between tension-compression and shear strains reported in [4]. Using the Fatemi-Socie (FS) parameter reasonable correlations were observed for the fatigue behavior of SAE 1045 steel under the four strain paths.

Several non-proportional strain paths were tested on 1%Cr-Mo-V steel by Jordan et al. [5] in order to investigate the relation between normal and shear strain during the fatigue process. Strain paths consisted of cyclic shear strain along with pulsating tensile and compressive strains with 1/10 frequency of the shear strain channel. A version of Wang-Brown parameter [6, 7] with few modifications was used to take into account the effect of interaction. Although correlations between tests with different strain paths were obtained by using two empirical material constants, lack of accounting for high frequency normal strain pulses and mean stress effects were among the weaknesses mentioned by the authors.

A critical plane approach based on modifying the Manson-Coffin fatigue properties was proposed by Wang and Susmel [8, 9] where a critical plane stress ratio was calculated based on the ratio between normal and shear stresses on the critical plane. The Modified Manson-Coffin Curve Method (MMCCM) was based on the concept that the shear fatigue properties used to correlate the shear strain amplitude to fatigue life are functions of the critical plane stress ratio. Therefore, for each multiaxial loading condition, different shear fatigue properties could be calculated and used to estimate the fatigue damage. Accurate predictions were reported in a number of studies containing test data under several stress and strain paths.

In the present study, a method is proposed to attempt to better account for the effect of interaction between normal and shear stresses. Based on the proposed method, a stress parameter was developed to represent the amount of this interaction for use in shear-based critical plane damage parameters containing both shear stress or strain and normal stress as input. Such critical planes are good candidates for the proposed method since they already account for the interaction by using both shear and normal components in estimating fatigue damage. Among different shear-based critical plane damage parameters, FS parameter [14], presented below, has been shown to successfully correlate test data under constant and variable amplitude multiaxial loads of different materials and components in many studies. This parameter was, therefore, selected for the implementation of the proposed method, given by:

$$\frac{\Delta\gamma_{max}}{2}\left(1+k\frac{\sigma_{n,max}}{\sigma_y}\right)=\frac{\tau_f'}{G}\left(2N_f\right)^{b_0}+\gamma_f'\left(2N_f\right)^{c_0} \tag{1}$$

Gates and Fatemi [15] recently suggested to replace σ_y by $G\Delta\gamma$, to better take the effect of high tensile mean stress into account. In this study, this form of FS damage parameter is used. A series of constant fatigue tests with irregular load paths consisting of different amounts of interactions between normal and shear stresses were designed. The results of these tests were used to investigate the ability of the proposed method in taking the effect of interaction into account. The designed load paths were then applied to a steel alloy, the Ti-6Al-4V titanium alloy, and the 2024-T3 aluminum alloy. The fatigue lives of these tests, as well as those found in the literature, were then used to evaluate the effectiveness of the proposed method.

2 The proposed method

There are two components of axial stress which can affect the fatigue damage process; the interaction normal stress, $\sigma_{n,int}$, which holds the faces of the crack open during alternating shear stresses, and the fluctuating normal stress, $\Delta\sigma_n$. The fluctuating normal stress can influence mode II short crack growth. Such detrimental mechanism for fluctuating normal stress has also been suggested in a study by Hoshide and Socie [16] where the Crack Sliding Displacement (CSD) was computed using functions which were calculated using both shear and normal stress components. Interaction of mode I cyclic loading with mode II growth of short cracks was also observed by Wong et al. [17, 18] in the analysis of tests on BS 11 normal grade rail steel under sequential plus-shaped loadings.

According to Doquet and Pommier [19] the effect of mode I loading on mode II growth for small amounts of normal stress is mainly due to periodically unlocking crack surfaces to increase the effect of mode II loading. For higher amounts of mode I loading, a synergetic effect due to the increase of plastic deformation and normality of plastic flow on the crack tips which leads to a rising biaxial ratcheting is also responsible for the interaction effects. In FS damage parameter, the effect of normal stress on the fatigue behavior is taken into account by an influencing factor which consists of the maximum normal stress on the shear plane and a material dependent constant. In other words, the two different mechanisms of the effect of normal stress are both taken into account by the maximum normal stress, which is the summation of mean and alternating stress.

The first damage mechanism of normal stress in the proposed method in this work is applied during the alternating shear stress. If tensile, this component of normal stress contributes to the fatigue damage by holding the faces of the small cracks open and facilitating the small crack growth process (i.e. reducing roughness-induced closure during shear crack growth). If compression, this component of normal stress holds the faces of the small crack closed and causes crack growth retardation. However, in order for this type of damage to be effective, the normal stress should be applied during alternating shear stress. The following is then the suggested term to represent this type of damage in the damage parameter:

$$\sigma_{n,int} = \frac{\int^T \sigma_n(t)|d\tau|}{2\int^T |d\tau|} = \frac{\int^T \sigma_n(t)\left|\frac{d\tau}{dt}\right|dt}{2\int^T \left|\frac{d\tau}{dt}\right|dt} \tag{2}$$

in which T is the time period of a cycle or reversal and $\sigma_n(t)$ is the normal stress history during this time period.

It can be seen that the interaction stress, $\sigma_{n,int}$, is calculated by integrating the normal stress over the periods of time when the shear stress is alternating. During the times when shear stress does not change, dτ is zero and, therefore, the normal stress does not contribute to the integral. It can also be observed that the interaction stress is calculated by averaging the normal stress over the changes in shear stress. It should also be noted that the direction of the shear stress does not influence fatigue damage since the normal stress has its effect on the fatigue behavior as long as shear stress is changing regardless of whether the change in shear stress is negative or positive. Hence, the absolute value of change in shear stress is used in Eq. (2).

Furthermore, the factor of two in the denominator of $\sigma_{n,int}$ was found to result in the most reasonable correlation for all of the analyzed materials and load paths. This factor can be explained by the mechanism of interaction which $\sigma_{n,int}$ represents. As mentioned earlier, the fluctuating component of the normal stress, $\Delta\sigma_n$, is also responsible for reducing the friction between the faces of the small cracks by periodically unlocking crack surfaces. Therefore, in modeling the fluctuating component of the normal stress, the effect on roughness-induced closure is also accounted for, which results in a smaller effect contributed by $\sigma_{n,int}$.

The fluctuating component of normal stress which is the second damage mechanism of normal stress can be simply represented as the range of the tensile part of the normal stress:

$$\Delta\sigma_n = \sigma_{n,max}\,\mathrm{H}\big(\sigma_{n,max}\big) - \sigma_{n,min}\,\mathrm{H}\big(\sigma_{n,min}\big) \tag{3}$$

where $\sigma_{n,max}$ and $\sigma_{n,min}$ are maximum and minimum normal stress, respectively, throughout a cycle or reversal and H(x) is Heaviside function which returns 1 for positive values and zero for negative values of x. It can be observed that whenever $\sigma_{n,max}$ and $\sigma_{n,min}$ are tensile, their values are accounted for in Eq. (3). However, since the compressive portions of the fluctuating normal stresses do not affect short crack growth in mode II, whenever the values of $\sigma_{n,max}$ or $\sigma_{n,min}$ are negative, H($\sigma_{n,max}$) or H($\sigma_{n,min}$) will result in zero, respectively. The summation of the effects of the two mechanisms can be used as the effect of the normal stress on fatigue damage, therefore:

$$\frac{\Delta\gamma_{max}}{2}\left(1 + k\,\frac{\sigma_{n,int}+\Delta\sigma_n}{G\Delta\gamma}\right) = \frac{\tau_f'}{G}\big(2N_f\big)^{b_0} + \gamma_f'\big(2N_f\big)^{c_0} \tag{4}$$

3 Experimental program

In the present study, one steel alloy, one titanium alloy, and one aluminum alloy were used for the experimental program. The selected steel alloy was 44MnSiVS6 which is used in the crankshaft of automotive engines. The selected titanium alloy was grade 5 Ti-6Al-4V and the selected aluminum alloy was 2024-T3, both of which are among the most commonly used alloys in the aerospace industry. Tubular specimens with wall thickness of 1.25 mm, inside diameter of 12.7 mm, and outside diameter of 15.2 mm were made from these materials.

The 44MnSiVS6 steel specimens were hot forged, controlled cooled, and machined, while the Ti-6Al-4V specimens were machined from pre-annealed bars. The aluminum specimens were machined from drawn tubing. The aluminium specimens were also tested using another geometry with wall thickness of 1.5 mm, inside diameter of 26 mm, and outside diameter of 29 mm. The tubular specimens were designed according to the criteria specified in ASTM Standard E2207 [20].

Table 1 presents the monotonic, cyclic deformation, and fatigue properties of the materials tested in this study. Details of the monotonic, cyclic deformation, and constant amplitude fatigue tests performed on the 44MnSiVS6 steel, Ti-6Al-4V titanium, and 2024-T3 aluminum can be found in [21], [22], and [15], respectively. In addition, Gates and Fatemi [15] also performed torsion fatigue tests with static axial stress as well as fatigue tests with triangular paths on 2024-T3 aluminum alloy specimens which were also analysed and used in the present study.

In order to investigate the effect of interaction between normal and shear stresses, different stress/strain paths with different levels of interaction between normal and shear stresses were designed and used in the experimental program. These paths are shown in Fig. 1. Path Z, shown in Fig. 1(a), has the least interaction between normal stress and shear strain. In this path, the shear cycle which is the primary cause of damage occurs without any axial stress. The shear cycle is then followed by axial stress cycles which are applied when the shear cycle is stopped. On the other hand, path T1 shown in Fig. 1(b) is consisted of a shear cycle which occurs when there is a static tensile stress applied and is followed by a cycle of axial stress which, similar to path Z, is applied when the shear cycle is stopped. Therefore, in this path both detrimental mechanisms of normal stress are active. Path T2 shown in Fig. 1(c) is similar to path T1. However, in path T2 there are two cycles of axial stress applied in the middle of each shearing reversal. Therefore, while only one shear reversal in path T1 is affected by the two detrimental mechanisms of normal stress, both shear reversals of path T2 experience these damaging mechanisms. As a result, if reversal counting is employed, path T2 causes more damage than path T1. Furthermore, tests found in the literature using a triangular path, shown in Fig. 1(d), and pure torsion path with static tensile stress, shown in

Fig. 1(e), were also analyzed in this study. These paths were used by Gates and Fatemi [18] for tests on 2024-T3 aluminum specimens.

Table 1. Monotonic, cyclic, and fatigue properties of 44MnSiVS6 steel, Ti-6Al-4V, and Al 2024-T3.

Property		**44MnSiVS6**	**Ti-6Al-4V**	**Al 2024-T3**
Axial and Shear Monotonic				
Modulus, GPa	E/G	209.2/80.3	108.2/42.0	73.7/27.4
Yield Strength, MPa	σ_y/τ_y	623.4/367.3	944/523.3	330/-
Ultimate Strength, MPa	σ_u/τ_u	959.7/-	1045/-	495/-
True Fracture Ductility, %	ε_f/γ_f	30.1/-	24.7/-	-/-
Strength Coefficient, MPa	K/K_0	1514/628	1253/595.7	470/-
Strain Hardening Exponent	n/n_0	0.147/0.087	0.051/0.021	0.055/-
Reduction in Area, %	$\%RA$	26.0	21.9	-
Elongation, %	$\%EL$	13.8	19.2	19.5
Axial and Shear Cyclic				
Cyclic Strength Coefficient, MPa	K'/K'_0	1270/655.8	878.2/511.1	677.0/382.3
Cyclic Strain Hardening Exponent	n'/n'_0	0.115/0.099	0.034/0.034	0.070/0.084
Cyclic Yield Strength, MPa	S'_y/τ'_y	621.3/354.5	710.9/413.8	415/266.8
Fatigue				
Fatigue Strength Coefficient	σ'_f/τ'_f	1188/610.6	987.1/646.7	1194/439.3
Fatigue Strength Exponent	b/b_0	-0.070/-0.053	-0.034/-0.044	-0.133/-0.078
Fatigue Ductility Coefficient	ε'_f/γ'_f	2.013/0.486	0.569/0.352	0.066/0.834
Fatigue Ductility Exponent	c/c_0	-0.737/-0.539	-0.636/-0.502	-0.445/-0.705

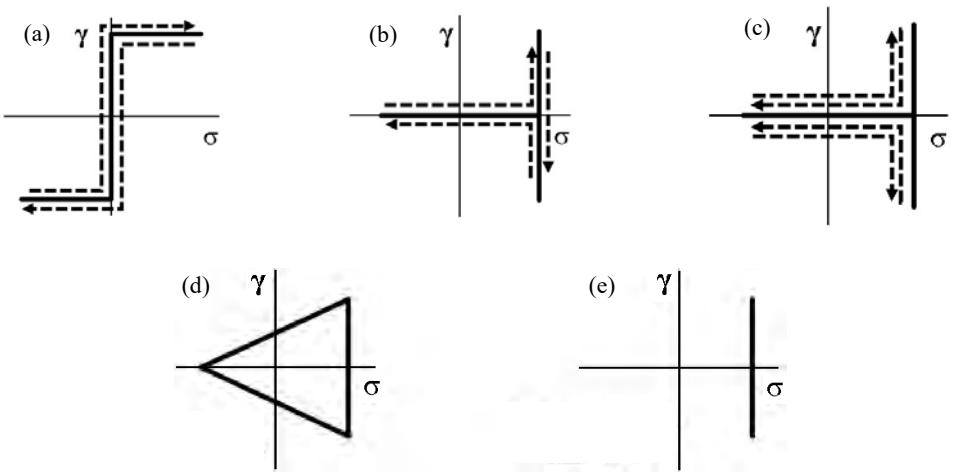

Fig. 1. Constant amplitude unconventional load paths designed to investigate normal and shear stress interaction effect; (a) path Z, (b) path T1, (c) path T2, (d) triangular path [18], and (e) torsion with static axial stress [18].

4 Analysis and results

Axial stress and shear strain, as well as the experimental fatigue lives of constant amplitude tests are shown in Table 2. It should be noted that the normal stress and shear strain levels of the tests on Ti-6Al-4V and 2024-T3 aluminum specimens were chosen in a way to generate similar fatigue lives without the proposed method. For 44MnSiVS6 Steel, however, the normal stress and shear strain levels are similar between different load paths. As expected,

for all materials fatigue lives of tests with path Z were longer than those of tests with paths T1 and T2. For instance, while path Z for Ti-6Al-4V specimens resulted in an average fatigue life of around 50,000 cycles, the tests with path T1 and T2, which had the highest interaction between normal and shear stresses, resulted in average fatigue lives of 28,000 cycles and 5,003 cycles, respectively. Although to a lesser degree, this was observed for tests on 44MnSiVS6 Steel as well. However, due to significant scatter observed in tests on 2024-T3 aluminum specimens, it is not clear whether tests with paths T1 and T2 had fatigue lives shorter than those with path Z. This scatter is specially observed in fatigue lives of tests with path T1.

Table 2. Experimental fatigue life results of the constant amplitude load paths (all lives are in number of cycles).

Material	Load path	σ_a (MPa)	γ_a (%)	Experimental life
44MnSiVS6 Steel	Path Z	350	0.350	28,400 37,313
	Path T1	350	0.350	17,760 22,000
	Path T2	350	0.350	16,100
Ti-6Al-4V	Path Z	455	0.714	40,701 58,680
	Path T1	500	0.785	26,647 29,303
	Path T2	500	0.785	5,003
Al 2024-T3	Path Z	170	0.420	21,129 29,511
	Path T1	180	0.440	4,724 4,776 18,206 20,000
	Path T2	180	0.440	17,746 27,015

As a means of comparison between the proposed method and the conventional method of using maximum normal stress, the ratio of the two values is plotted against the experimental fatigue life. This plot, shown in Fig. 2(a) contains test data of conventional constant amplitude fatigue tests including axial, torsion, combined in-phase, and combined 90˚ out-of-phase, along with the unconventional paths shown in Fig. 1. As observed, for the conventional fatigue tests, the proposed method results in the same amount of influencing normal stress as maximum normal stress. However, for paths T1 and T2, as well as the torsion tests with static axial load and tests with triangular paths performed in [15], the proposed normal stress term is higher than the maximum normal stress.

Furthermore, the results of the fatigue life estimation of the constant amplitude fatigue tests with unconventional paths along with both cycle and reversal counting are shown in Figs. 2(b) and 2(c), respectively. As expected, fatigue life estimations of tests with paths Z and T1 are similar between cycle and reversal counting. Moreover, it can be observed that fatigue tests with path T1 have shorter estimated lives compared to those with path Z. However, the calculated fatigue damages of these paths are without the propose modification.

Fig. 2 also shows that, as mentioned earlier, using reversal counting results in higher damage calculated for path T2, as compared to path T1. While for each material estimated fatigue lives of paths T1 and T2 are similar if cycle counting is used, reversal counting results

in a factor of 2 difference between these estimations. This is because only one reversal in path T1 contains the damage from fluctuating tensile stress. Overall, it was observed that the proposed method along with either cycle or reversal counting resulted in reasonable estimation of fatigue lives for the tests with unconventional constant amplitude paths as nearly all the data fell in scatter bands of ±3. Fatigue lives of torsion tests with static axial load and tests with triangular paths performed in [15] were also reasonably estimated.

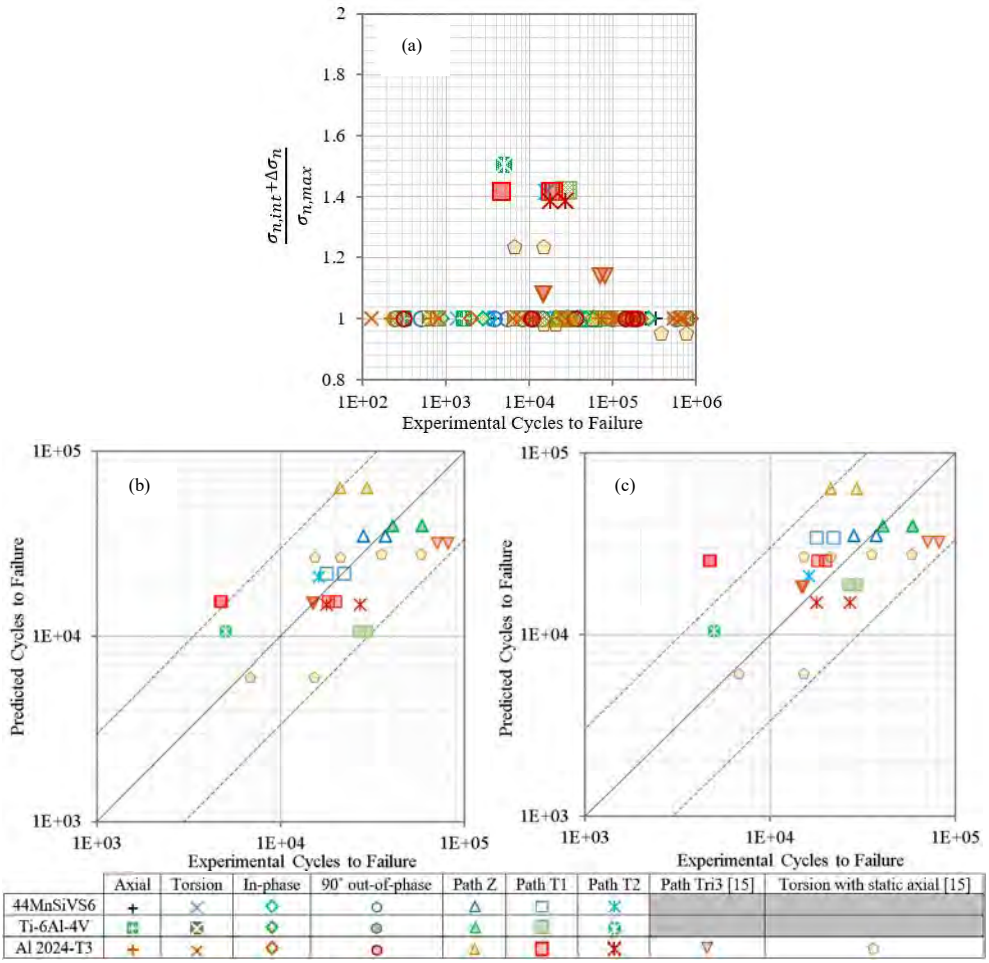

Fig. 2. (a) Ratio of the summation of the normal stress parameters used in the proposed method to the maximum normal stress plotted against the experimental fatigue lives of constant amplitude fatigue tests, as well as predicted vs. experimental fatigue lives of unconventional constant amplitude fatigue tests using (b) cycle counting and (c) reversal counting.

Furthermore, the failure orientations observed on the 44MnSiVS6 steel, Ti-6Al-4V titanium, and 2024-T3 aluminum specimens under the tested paths were reasonably predicted with the proposed method. Fig. 3 shows the observed orientations of crack initiation plotted against the predicted failure orientations. As shown, almost all crack initiation orientations were predicted within 10˚ from the experimental observations. To investigate the application of the proposed method to more realistic service loadings, this method was also used with three multiaxial variable amplitude histories applied to 44MnSiVS6 steel and Ti-6Al-4V titanium alloy, the results of which are presented and discussed in [23].

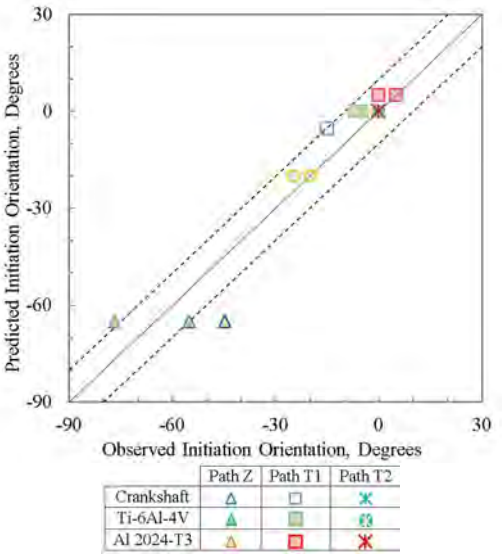

Fig. 3. Observed initiation orientations of tests with unconventional constant amplitude load paths plotted vs. predicted initiation orientations.

5 Summary and conclusions

This study investigated the effect of interaction between normal and shear stresses on multiaxial fatigue behavior. A method was proposed to account for the interaction which could be used in shear-based critical plane damage models. This method was applied to the FS damage parameter. A series of constant amplitude tests were designed for three metallic materials to investigate the effect of interactions between normal and shear stresses the results of which were analysed by the proposed method. For two of the materials which did not show excessive scatter, it was observed that load paths with high interactions between tensile and shear stresses resulted in shorter fatigue lives as compared to those without significant interactions. The proposed method resulted in reasonable correlation of test data in terms of fatigue life as well crack plane orientation.

References

1. R.I. Stephens, A. Fatemi, R.R. Stephens, and H.O. Fuchs, *Metal fatigue in engineering,* John Wiley & Sons, (2000)
2. H.C. Wu, C. Yang, "On the influence of strain path in multiaxial fatigue failure." J. Eng. Mater. Technol., **109**, 107-115 (1987)
3. P. Kurath, Y. Jiang, and A. Fatemi, "Strain-path influence on multiaxial deformation and fatigue damage." SAE AE-28, 117-140 (1999)
4. S. Subramaninan, A. Fatemi, "Strain-path influence on multiaxial fatigue cracking." *Proceedings of the Fourth International Conference on Fatigue and Fatigue Thresholds*, **1**, 399-404 (1990)
5. E. H. Jordan, M.W. Brown, and K.J. Miller, "Fatigue under severe nonproportional loading." *Multiaxial fatigue, ASTM International*, 569-585 (1985)

6. C. Wang, M. Brown, "A path-independent parameter for fatigue under proportional and non-proportional loading." Fatigue. Fract. Eng. Mater. Struct., **16(12)**, 1285-1297 (1993)

7. C. Wang, M. Brown, "Life prediction techniques for variable amplitude multiaxial fatigue—part 1: theories." J. Eng. Mater. Technol., **118(3)**, 367-370 (1996)

8. Y. Wang, L. Susmel, "The Modified Manson–Coffin Curve method to estimate fatigue lifetime under complex constant and variable amplitude multiaxial fatigue loading." Int. J. Fatigue., **83**, 135-149 (2016)

9. L. Susmel, G. Meneghetti, and B. Atzori, "A simple and efficient reformulation of the classical manson–coffin curve to predict lifetime under multiaxial fatigue loading—part I: Plain materials." J. Eng. Mater. Technol., **131(2)**, 021009 (2009)

10. Y. Wang, N.Z. Faruq, and L. Susmel, "Evaluation of different techniques in estimating orientation of crack initiation planes and fatigue lifetime under complex multiaxial loading paths." Int. J. Fatigue., **100**, 521-529 (2017)

11. K. Kim, J. Park, and J. Lee, "Multiaxial fatigue under variable amplitude loads." J. Eng. Mater. Technol., **121(3)**, 286-293 (1999)

12. N. Shamsaei, A. Fatemi, and D.F. Socie, "Multiaxial fatigue evaluation using discriminating strain paths." Int. J. Fatigue., **33(4)**, 597-609 (2011)

13. N. Shamsaei, M. Gladskyi, K. Panasovskyi, S. Shukaev, and A. Fatemi, "Multiaxial fatigue of titanium including step loading and load path alteration and sequence effects." Int. J. Fatigue., **32(11)**, 862-1874 (2010)

14. A. Fatemi, D.F. Socie, "A critical plane approach to multiaxial fatigue damage including out-of-phase loading." Fatigue. Fract. Eng. Mater. Struct., **11(3)**, 149-165 (1988)

15. N. R. Gates, A. Fatemi, "On the consideration of normal and shear stress interaction in multiaxial fatigue damage analysis." Int. J. Fatigue., **100**, 322-336 (2017)

16. T. Hoshide, D. Socie, "Mechanics of mixed mode small fatigue crack growth." Eng. Fract. Mech., **26(6)**, 841-850 (1987)

17. S. Wong, P. Bold, M. Brown, and R. Allen, "A branch criterion for shallow angled rolling contact fatigue cracks in rails." Wear, **191(1-2)**, 45-53 (1996)

18. S. Wong, P. Bold, M. Brown, and R. Allen, "Fatigue crack growth rates under sequential mixed-mode I and II loading cycles." Fatigue. Fract. Eng. Mater. Struct., **23(8)**, 667-674 (2000)

19. V. Doquet, S. Pommier, "Fatigue crack growth under non-proportional mixed-mode loading in ferritic-pearlitic steel." Fatigue. Fract. Eng. Mater. Struct., **27(11)**, 1051-1060 (2004)

20. ASTM-E2207-15, "Standard practice for strain-controlled axial-torsional fatigue testing with thin-walled tubular specimens." *Annual Book of ASTM Standards*, **03.01** (2017)

21. S. Sharifimehr, A. Fatemi, "Fatigue analysis of ductile and brittle behaving steels under variable amplitude multiaxial loading." Fatigue. Fract. Eng. Mater. Struct. 1-21 (2019)

22. A. Fatemi, R. Molaei, S. Sharifimehr, N. Phan, and N. Shamsaei, "Multiaxial fatigue behavior of wrought and additive manufactured Ti-6Al-4V including surface finish effect." Int. J. Fatigue., **100**, 347-366 (2017)

23. S. Sharifimehr, A. Fatemi, "On the interaction of normal and shear stresses in multiaxial fatigue damage." Fatigue. Fract. Eng. Mater. Struct., accepted (2019)